Biomechanics of the peafowl's crest: a potential mechanosensory role for feathers during social displays

Suzanne Amador Kane*[1], Daniel Van Beveren[1], Roslyn Dakin[2,3]

[1] Physics Department, Haverford College, Haverford, PA 19041, USA
[2] Department of Zoology, University of British Columbia, Vancouver, BC V6T1Z4, Canada
[3] Migratory Bird Center, Smithsonian Conservation Biology Institute, P.O. Box 37012, Washington, DC 20013, USA

*corresponding author: samador@haverford.edu

Running title: Biomechanics of peafowl feather crests

Keywords: plumage; mechanoreception; vibration; resonance; near-field sensing; peacock; multi-modal signaling

Summary statement: Avian crest feathers have mechanical properties that make them suitable for sensing airflows generated during multimodal social displays.

ABSTRACT

Feathers act as vibrotactile sensors that can detect mechanical stimuli during avian flight and tactile navigation, suggesting that they may also function to detect signals during social displays. We explored this novel sensory modality using the crest plumage of Indian peafowl (*Pavo cristatus*). We first determined whether the airborne stimuli generated by peafowl courtship and social displays couple efficiently via resonance to the vibrational response of feather crests from the heads of peafowl. Peafowl crests were found to have fundamental resonant modes with frequencies that could be driven near-optimally by the shaking frequencies used by peafowl performing train vibrating displays. Crests also were driven to vibrate near resonance when audio recordings of sounds generated by these displays were played back in the acoustic near-field, where such displays are experienced *in vivo*. When peacock wing-shaking courtship behaviour was simulated in the laboratory, the resulting directional airflow excited measurable vibrations of crest feathers. These results suggest that peafowl crests have properties that make them suitable mechanosensors for airborne stimuli generated during social displays. Such stimuli could complement acoustic perception, thereby enhancing detection and interpretation of social displays. Diverse feather crests are found in many bird species that perform similar displays, suggesting that this proposed sensory modality may be widespread, and possibly derived from flow sensing in other contexts. We suggest behavioral studies to further explore these ideas and their functional implications.

INTRODUCTION

A large body of research in mammals and insects has found that whiskers, antennae, and cerci play important sensory roles directly related to their vibrational response and mechanical structures (Barth et al., 2012; Sofroniew and Svoboda, 2015). The similar morphology of elongated facial feathers in birds raises the question of whether feathers might serve a similar somatosensory function (Seneviratne and Jones, 2008; Seneviratne and Jones, 2010). Indeed, feather crests and whisker-like plumes are found in a wide variety of bird species encompassing many different orders (Seneviratne and Jones, 2010). Most studies of elongated head feathers have focused on their possible role as sexually- or socially-selected traits during courtship and dominance interactions (Burley and Symanski, 1998; Hagelin, 2002; Jones and Montgomerie, 1992). However, bird feathers are often coupled to vibration-sensitive nerve endings that can allow birds to sense and respond to a variety of mechanical stimuli (Brown and Fedde, 1993; Necker, 1985; Saxod, 1978). Thus, feathers can act as lightweight sensors that provide important information during flight (Bilo and Bilo, 1978; Brown and Fedde, 1993; Brücker et al., 2016), tactile navigation (Seneviratne and Jones, 2008; Seneviratne and Jones, 2010), and prey capture (Cunningham et al., 2011). Indeed, feathers may have evolved to serve such sensory functions before the evolution of other functions such as thermoregulation and flight (Persons and Currie, 2015).

During social displays, many birds also perform behaviors that generate mechanical cues (Clark, 2016). Motions such as flapping or vibrating the wings or tails can produce sounds, airflow patterns, and substrate vibrations that could function as signals (Bostwick et al., 2009; Clark et al., 2013; Dakin et al., 2016; Ota et al., 2015). These multimodal displays may stimulate multiple senses, including visual, acoustic and vibrotactile perception. For example, male Indian peafowl ("peacocks", *Pavo cristatus*) attract mates by spreading and erecting the train, a fan-like array of long, colorful feathers, and performing two different shaking behaviors. First, in the wing-shaking display, the peacock orients his backside toward nearby females and flaps his partially unfurled wings at approx. 5.4 Hz. Second, in the train-rattling display, the peacock faces a female at close range (approx. 1 to 1.5 m) and shakes his tail and train feathers rapidly at 22-28 Hz (mean = 25.6 Hz), causing his train to shimmer iridescently and emit a mechanical sound (Dakin and Montgomerie, 2009; Dakin et al., 2016; Freeman and Hare, 2015). Train-rattling performance by peacocks is obligatory for mating success (Dakin and Montgomerie, 2009), and eye-tracking experiments have shown that both wing-shaking and train-rattling displays are effective at attracting and holding the peahen's gaze (Yorzinski et al., 2013). Peahens also perform a tail-rattling display at 25-29 Hz in a variety of contexts (Dakin et al., 2016), suggesting that feather vibrations might serve other communicative functions as well. Peafowl can detect audio playback of train-rattling and wing-shaking recordings filtered to remove frequencies > 20 Hz and played back at large distances (5 m) (Freeman and Hare, 2015).

The sound generated by animal motions can be thought of as consisting of oscillations in both air pressure and velocity (Fletcher, 1992; Larsen and Wahlberg, 2017). The most familiar scenario, called the far-field, occurs when the distance, R, between the source and receiver is large compared to both the wavelength of sound, λ, and the size of the source, A (i.e., $R >> \lambda$ and $R >> A$). In the far-field, pressure waves dominate and amplitude (sound pressure level or SPL) varies as $1/R$ and power decreases as $1/R^2$, corresponding to an SPL decrease by -3 dB and a power decrease of -6 dB when R doubles. The near-field corresponds to the case when either of

two criteria hold: when the wavelength exceeds R ($R \lesssim \lambda$; e.g., this can occur for low frequencies characteristic of locomotion or motions during displays when receivers are nearby the sender), or when the source (e.g., shaking appendages such as wings, trains or tails) size is comparable to or exceeds R ($R \lesssim A$; e.g., this can occur when the receiver is close to the sender compared to the size of shaking appendages such as wings, trains or tails). In the near-field regime, particle velocity dominates at very small R and the decrease in both pressure and velocity depends on exact source characteristics. While there is no hard distinction between the near- and far-fields, the pressure contribution gradually increases relative to the velocity field as the far-field limit is approached. Research on low-frequency vibrational communication mostly has focused on substrate-borne signals and relatively few studies have considered near-field vibrotactile reception of near-field air-borne signals. Near-field communication has been studied in aquatic animals, including crustaceans, fish, and whales (Bradbury and Vehrencamp, 2011; Butler and Maruska, 2016; Mooney et al., 2016), as well as a wide variety of invertebrate taxa (Markl, 1983). In arthropods, near-field airborne signals are detected via tactile as well as auditory means, and many species use filiform hairs to detect near-field air velocity for predator or prey detection and, in some cases, intraspecies signaling (Barth, 2014; Santer and Hebets, 2008). It is not yet known whether birds also use non-auditory senses to detect near field velocity (airflow patterns) during social displays, or what influence this may have on their social interactions.

One possible means by which peafowl may sense potential near-field signals is the fan-like crest, a planar array of feathers oriented in the sagittal plane that is found on the heads of both male and female peafowl (Dakin, 2011). Each crest feather has a long shaft (rachis) with short, sparse barbs along its length, and a spatula-shaped "flag" of pennaceous vanes at the distal end (Fig. 1). Although it has been proposed that the peafowl crest may serve as a signal of status (Dakin, 2011), the crest feather morphology is similar to that of filoplumes, a type of feather with known mechanical sensitivity (Alibardi, 2009; Lucas and Stettenheim, 1972; Seneviratne and Jones, 2008) that protrude on the face and head of many bird species. This suggests that the crest may have a somatosensory function. Moreover, because the peafowl's region of most acute vision is oriented laterally (Hart, 2002), when a peahen gazes at a displaying male, the maximum area of her crest feathers also points toward the peacock's moving feathers. This results in the optimal orientation for responding to air motions generated by the displaying bird (Fig. 1A).

With this background in mind, we explored the biomechanics of the peafowl crest and its potential role as a sensor during peacock displays. We would expect bird feathers to have certain biomechanical properties in order for them to function effectively as tactile airflow sensors. In particular, they should vibrate efficiently at socially salient frequencies, either to detect shaking by a conspecific individual, or as a form of proprioception to provide feedback to the animal doing the shaking (Dambach et al., 1983; Kämper and Dambach, 1981). This can be accomplished readily via mechanical resonance, the phenomenon whereby an object responds with maximum amplitude to a driving force that oscillates at one of its natural frequencies of vibration (Smith, 2010). Thus, we expect the feather crests to have a vibrational resonant mode that can be excited by the frequencies and motions used during social displays, as is the case for the feathers used to perform such displays (Bostwick et al., 2009; Clark et al., 2013; Dakin et al., 2016). To test this hypothesis, we used video-based vibrometry (Davis et al., 2015) to measure the resonant frequencies of peafowl feather crests and individual crest feathers, and compared

them with *in vivo* train- and tail-rattling shaking frequencies (Dakin et al., 2016). Because interactions between feathers can influence the resonant frequency and damping, we also compared the biomechanics of crests to that of isolated feathers (Cummins and Gedeon, 2012). To test whether mechanical sound might cause crest motion in females located in the near-field of train-rattling peacocks, we measured deflections of crests that were exposed to audio playbacks in the laboratory of train-rattling and a white noise control.

Next, we considered the peacock's wing-shaking display. Because avian wing flapping during flight is known to shed vortices periodically, we hypothesized that the wing-shaking display would also result in periodic airflow disturbances that could drive significant crest feather motion. To test this hypothesis, we used a peacock wing-flapping robot to visualize the response of peafowl crests to airflow produced during simulated wing-shaking displays. Together, these experiments provide a first step to evaluating the potential mechanosensory responses of the avian crest during social signalling. We discuss how this can be followed with further behavioral experiments on live animals.

MATERIALS AND METHODS

In vitro samples

All measurements and fitted values are reported as means [95% confidence interval] unless noted otherwise. A total of n = 7 male and n = 8 female Indian peafowl (*Pavo cristatus* Linnaeus 1758) head crests with the feathers still mounted in skin were purchased from commercial vendors. Length and width measurements were made by hand and from digital photographs of crests and high-resolution scans of single feathers with a ruler included in the sample plane (Fig. 1). All male crest samples had feathers of uniform length (±8%), whereas the female crest samples had, on average, 7.0% [2.1, 11.8] of their feathers appreciably shorter than the maximum length of the crest. Eight out of 15 crests had all feathers oriented in the same plane within ±5º; five of the crests had 7-11% of the feathers unaligned, and two male crests had 22% and 50% unaligned feathers, respectively. We used photographs from a previous study (Dakin, 2011) that included a scale to compare the morphology of *in vitro* samples here to that of the crests on live birds. The morphological traits compared included length, width and number of feathers.

For mechanical testing, we glued the lower side of the crest skin to a ~2.5 cm cube of balsa wood using hot glue (Fig. 1C). An earlier study that compared the resonance of peacock feathers mounted using rigid balsa wood mounts versus a compliant gel found that the compliant mounts resulted in only slightly lower resonant frequencies and reduced amplitudes at frequencies > 50 Hz (Dakin et al., 2016). If the crest feathers were closely clustered, the attached skin was first softened in water and the crest was spread to approximate its natural configuration. To study individual, isolated feathers, we removed all but three feathers (one on each outer edge and one in the middle) from two male and two female crests, and analyzed the characteristics of those remaining feathers.

Vibrational dynamics trials

For vibrational dynamics measurements, the feather assembly was mounted on a model SF-9324 mechanical shaker (Pasco Scientific, Roseville, CA, USA) driven by an Agilent 33120A function generator (Agilent Technologies, Wilmington, DE, USA) (Fig. S1). Two orthogonal directions of the driving force were used: "out-of-plane", oriented normal to the plane of the crest; and "in-plane", oriented parallel to the plane of the crest and in the posterior-anterior axis of the head (Fig. 1C). The first orientation (out-of-plane) corresponds to the geometry when a peafowl either visually fixates the display by orienting one side of the head towards it, or else drives its own crest into vibrations by performing a train- or tail-rattling display (Dakin et al., 2016). The second (in-plane) orientation recreates the geometry when the front of the head is oriented towards the display or when the bird bobs its head during feeding or walking. The vibrational response spectrum was measured using three linear frequency sweeps with rates validated by an earlier study of peafowl displays and feather vibrational properties (Dakin et al., 2016): 0.042 Hz s^{-1} over 0.5–3.0 Hz; 0.25 Hz s^{-1} over 0–15 Hz; and 1.8 Hz s^{-1} over 10–120 Hz. Each of the 15 crests was tested three separate times in the out-of-plane orientation at the 0-80 Hz frequency range (n = 45 trials). We also ran additional trials, as follows: six crests out-of-plane at 0-120 Hz (n = 18 trials), five crests in-plane at the 0-80 Hz range (n = 14 trials), and two crests in-plane at 0-120 Hz (n = 2 trials).

Video analysis

We recorded feather vibrational motions using high-speed video filmed with a GoPro Hero 4 Black Edition camera (720 x 1280 pixels; 240 frames s^{-1}; GoPro, San Mateo, CA, USA). Image and data analysis were performed using custom programs based on the Matlab 2015a Machine Vision and Fitting toolboxes (MathWorks, Natick, MA, USA) available on figshare (Dakin et al., 2017). To analyze feather motion, we first used auto-contrast enhancement and thresholding to track separately the mean position of the crest feather flags and shaker mount vs. time, and then computed the spectrogram of each object's tracked position during the frequency sweep using a Hanning filter. This yielded the magnitude, A, of the fast Fourier transform (FFT) at each vibrational drive frequency, f_d, which was divided by the shaker drive magnitude, A_d, at that frequency to give the drive transfer function (A/A_d). Finally, the drive transfer function was smoothed over a 1.3 Hz window using a cubic Savitzky-Golay filter and all peaks in the response were fit to a Lorentzian function using nonlinear-least squares fitting to obtain the resonant frequency, f_r, and full-width-half-maximum, Δf, of the spectral power (Smith, 2010). These fits were performed in Origin 8.6 (Originlab, Northhampton, MA, USA). The quality factor, Q (a measure of how sharply defined in frequency the resonance is), was computed from $Q = f_r/\Delta f$.

Audio playback experiments and analysis

To determine if peafowl crests move detectably due to the near-field airflow of train-rattling vibrations, we filmed high-speed video of one female and one male feather crest in the near-field of a speaker playing audio recordings of peacock train-rattling displays. Two types of playback stimuli were used: (1) three different train-rattling sequences recorded in the field in a previous study (Dakin et al., 2016) from three different displaying peacocks, with mean rattle frequencies of 25.0 ± 1.0 Hz; 25.5 ± 0.6 Hz; and 24.6 ± 0.8 Hz; and (2) white noise generated by Audacity (audacityteam.org; downloaded June, 2017). To ensure that playbacks were in phase over several seconds, sequences lasting approximately 1.2 s long were edited to contain an integer number of rattling periods, and combined to make up a 30 s long audio file.

Audio recordings were played on a personal computer and amplified using a model 402-VLZ3 mixer (Mackie, Woodinville, WA, USA) and model 120 servo amplifier (Samson Technologies, Hicksville, NY, USA). An earlier analysis of peacock train-rattling mechanical sound indicated that these noises were broadband rattles emitted at a rate of ~26 Hz, as opposed to sound waves with spectral density predominantly in the infrasound (Dakin et al., 2016). We consequently used a model MR922 speaker (JBL Professional Products, Northridge, California) with a broadband response that had a 30 cm diameter low frequency driver mounted in an acoustically absorbing enclosure (± 10 dB over 60 Hz-17 kHz). Two crest samples (one male and one female) with resonant responses determined in the vibrational dynamics trials were studied by remounting each crest on a 0.64 cm thick square of plywood attached to a force plate. These samples were positioned 30 cm away from the 30 cm diameter speaker face to ensure that the samples were in the near-field. To confirm that the broadband nature of the audio resulted in no variation in intensity due to near-field interference, we measured average sound pressure levels (SPL) near the speaker using a model JTS1357 sound level meter (range: 31.5 Hz-8.5 kHz; ± 2 dB accuracy; A-weighting) (Sinometer, Shenzhen, China). No variation was found within measurement error (± 0.3 dB SPL) at five locations across the speaker's face vertically and horizontally and perpendicular to the speaker face. Measurements taken when no audio was playing found audible frequency background SPL values of 54 ± 0.1 dB.

Relatively few values of the sound intensity generated by bird wing-flapping have been reported in the literature to use as references for this experiment. Peacock wing-shaking sound levels for frequencies ≤ 20 Hz were reported as 73-79 dB SPL at 4 m, which extrapolates to approx. 79-85 dB SPL at 1 m using far-field scaling (Freeman and Hare, 2015), whereas audible bird wing-beat sound levels for much smaller species were reported at 64-66 dB SPL and 54-60 dB SPL at 1 kHz and 25 kHz, respectively, at 1.2 m for Eastern phoebes (*Sayornis phoebe*) and chickadees (*Poecile atricapillus*) (Fournier et al., 2013) and ≤ 67.6 dB SPL at approx. 1.0 m for crested pigeons (*Ocyphaps lophotes*) (Hingee and Magrath, 2009), and ruffed grouse drumming (a wing-beating display) corresponded to 66.2 dB SPL at 1 m (Garcia et al., 2012). To compare our values with previous work, we Fourier-analyzed a recording of the playback made with a Sennheiser ME-62 microphone (±2.5 dB: 20 Hz to 20 kHz; Sennheiser, Wedemark, Germany). This indicated that the component of the power spectrum of the playback near the crest resonance was only 3.5-11% of the total playback power. Thus, while sound levels measured for the audio playbacks in the human audible range were approx. 90-97 dB SPL, we estimate that the component due to frequencies near resonance were much lower, approx. 75-87 dB SPL (-10 log (3.5 to 11%)).

To minimize direct mechanical coupling via the substrate between the speaker and the samples, we mounted the speaker separately on the floor and used a Sorbothane™ vibration-isolation pad under the optical breadboard holding the crest samples. Insertion of an acoustic foam tile between the feather crests and speaker to block airflow reduced the FFT spectral power at the resonant frequency of the crests to 6.5% of its value without the tile; the remaining background vibrations are due to background caused by substrate vibrations and reverberation, as well as any pressure waves transmitted through the foam. To find the background noise level due to environmentally driven vibrations for use in the Fourier analysis, we also measured crest vibrations in the absence of audio playbacks. The background FFT power spectrum peak showed a single peak at the resonant frequency with the same power either when measured with

no audio playing or when measured during lower intensity playbacks (≤ 75 dB at distances ≥ 30 cm).

Simulated wing-shaking experiments

High-speed videos from a previous study were used to determine the frequency and amplitude of wing motions during the peacock's wing-shaking display (Dakin et al., 2016); we used four videos with the correct perspective that also showed tail feathers with known lengths to estimate the mean diameter of wing motion circumscribed by the tips of the partly-unfurled wings during this display as 7.6 cm (range 5.5 to 10 cm; Fig. 4). To simulate the resulting air motions in the laboratory, we used a robotic mechanism that caused an actual peacock wing to move such that its plane remained in the same orientation while its distal end circumscribed a circle with the same rotational circulation as found in living birds (movie 1 and Fig. S2). The peacock wing was mounted on a carbon fiber rod using a balsa wood base that was attached to the wing via adhesive at the shoulder; this rod pivoted about a clevis joint, which allowed the wing axis to move in a vertical circle while the wingspan remained in the vertical plane. At the end opposite the wing, the rod was attached to a circular crank by a universal joint. The crank and attached wing assembly was driven at 4.95 ± 0.05 Hz by a DC motor. While actual wing-shaking involves motions of two wings toward each other, each with diameter 10 cm, which presumably displaces more air than a single wing, this apparatus used a single flapping wing moving in a slightly larger diameter (14 cm) circle at the wingtips.

To determine how wing-shaking influences the crest of an observing bird, we first determined the location of maximal airflow speed during robotic wing-shaking. Airflow speeds were measured by a model 405i Wireless Hot-wire Anemometer (Testo, Sparta, NJ, USA) oriented with its sensor facing in the same direction as the crest samples; this device has a resolution of 0.01 m/s, accuracy of 0.1 m/s, 1 Hz measurement rate, and approx. 5 s equilibration time. To define the airflow pattern around the flapping wing, air speed was sampled at every point on a 5 cm grid 5-7 times per location. Using to these results, wood-mounted peahen feather crests were positioned using a tripod at the vertical midline of the wing located at varying distances from the wing-tips as shown in Fig. S2. The resulting motions of the crests were then filmed using high-speed video as described above in "Video analysis" to quantify the vibrational response of three different peahen crests. To verify that substrate vibrations did not drive the crest motion, we performed a control by inserting a 3 x 4 ft foamboard in between the crest and wing to block the airflow from the wing motion; this reduced the root-mean-squared crest motion to 14% of its value with wing motion-induced airflow present. For comparison with the wing-shaking frequency during displays, flapping frequencies during ascending and level flight were also measured for 9 peacocks from 6 online videos (Table S1).

Air vortex experiments

To understand further the response of crests to individual airflow impulses, we used a Zero Blaster vortex gun (Zero Toys, Concord, MA, USA) to generate single air vortex rings of artificial fog (2-4 cm in diameter, 1 cm diameter cross-section, speed 1.8 m/s [95% CI 1.7, 2.0 m/s, range 1.5 - 2.1 m/s]), aimed so as to impact whole crests (n = 2 peacocks and 1 peahen crests) in the out-of-plane orientation. The motion of crest feathers struck by the vortices was measured by tracking the crest position on high-speed video when an intact vortex impacted the crest oriented with its widest cross-section facing the source at 0.5 m from the point of creation.

Force measurements

We studied the static mechanical response of peafowl crests in the single cantilever bending geometry by measuring the relationship between flag displacement and restoring force of the crest in the out-of-plane orientation (Fig. 1C). Force measurements were made using a Model DFS-BTA force sensor (accuracy ± 0.01 N) connected to a LabQuest2 datalogger (Vernier Software & Technology, Beaverton, OR, USA), which was calibrated using known masses. The force sensor was attached to a thin rectangular plastic blade oriented in the horizontal plane. The edge of the blade was pressed against the midpoint of the flags of the vertically oriented crest to measure the restoring force exerted by the bent crests. The crests were mounted on a micrometer which moved them toward the force sensor and enabled measurement of crest displacement relative to the location at which restoring force first became non-zero. The resulting force vs displacement data were fit to a linear model to determine the elastic bending constant, k, for three trials each for three male and three female crest samples.

For the air vortex and audio playback studies, the crest samples were mounted on a balsa wood block that was mounted on two vertically-oriented force probes at either end separated by 3.0 ± 0.1 cm. Since the flags are approximately 5 cm from the base, the mean force on the crest feather flag, F, can be computed from ΔF (the difference between the downward forces recorded by each sensor) using $F = (5/1.5)\ \Delta F = 3.3\ \Delta F$.

Statistical analysis

To analyze sources of variation in whole crest f_r and Q, we fit Gaussian linear mixed effects models with a random effect of crest ID to account for repeated measures of each bird's crest using the nlme package (Pinheiro et al., 2017) in R (R Core Team, 2017). We first verified that trial order and frequency sweep rate, two aspects of the experimental design, did not have significant effects on either f_r or Q (all $p > 0.28$). The next step was to evaluate the potential effects of morphological traits that could influence crest resonance. Because we had only 15 crests, we considered models with one morphological trait fixed effect at a time, selected from the following list of traits: length, width, number of feathers, percent of unaligned feathers, and percent of short feathers. All models also included fixed effects of the vibration orientation (in or out-of-plane), as well as sex. We used AICc to select the best-fit model (Bartoń, 2015) and evaluated significance of the fixed effects in that model using Wald tests. We report $R^2_{LMM(m)}$ as a measure of the total variance explained by the fixed effects (Bartoń, 2015; Nakagawa and Schielzeth, 2013). We used the variance components of the best-fit model to calculate the repeatability of measurements after accounting for variation explained by the fixed effects (Nakagawa and Schielzeth, 2010). Inspection of the data and model residuals revealed that variance in f_r differed among crests, so when modelling f_r, we specified this heteroscedasticity using the weights argument (Pinheiro et al., 2017).

RESULTS

Morphology

Fig. 1D shows that the range of lengths of dried feather crests measured in this study agreed with that of live peafowl, indicating that the crest samples used in the experiments were fully grown (Dakin, 2011). However, the widths of the mounted crests were approx. 20% (female) to 27%

(male) smaller than those found on live birds (Fig. 1D). This difference could be due to the crest ornament being spread 1-2 cm in the sagittal plane by muscle action in the live bird, similar to erectile crest plumage in many other species (Hagelin, 2002), in addition to the effect of skin drying.

We also studied the morphology of individual crest feathers to understand their unusual structure (Fig. 1E). The average rachis tapered evenly over its 39.90 [38.89, 40.91] mm length and had a mass of 5.1 [4.8, 5.3] mg, and the plume (or flag) added another 2.5 [0.87, 4.06] mg. Unlike the fully formed barbs in the pennaceous flag, the lower barbs were short (4.1 [3.0, 5.2] mm) and lacked barbules altogether.

Vibrational Dynamics

The vibrational drive transfer functions of peafowl crests had either a single dominant fundamental peak, or in a few cases a cluster of peaks in a narrowly-defined frequency range, with no evidence that other modes of vibration caused detectable motions of the pennaceous flags. Each main peak agreed well with the fitted Lorentzian function (mean adjusted-R^2 = 0.97; range [0.91, 0.998]). The value of $f_r \pm \Delta f/2$ defines the approx. range of drive frequencies over which power is efficiently coupled into the oscillator. Fig. 2 shows that shaking frequencies measured in the field for displaying male and female peafowl (Dakin et al., 2016) lay within $f_r \pm \Delta f/2$ for both sexes. For the shaking force oriented out-of-plane, the mean crest resonant frequency, f_r, was 28.07 [28.01, 28.14] Hz for female and 26.3 [25.9, 26.6] Hz for male crests, respectively. The mean Δf values were 6.2 [4.4,8.0] Hz (females) and 4.3 [4.2, 4.4] Hz (males).

Analysis of the sources of variation in f_r indicated that 28% of the variation in the resonant frequency could be explained by sex, crest orientation, and the total area of the pennaceous flags (Fig. 2). The effect of crest orientation was strong and significant, such that out-of-plane vibrations have approx. 2.4 Hz higher f_r on average ($p < 0.0001$), whereas the sex difference was not significant ($p = 0.87$) and crests with reduced flag area have a slight but non-significant tendency to have higher f_r values ($p = 0.10$). Although length, width, number of feathers, and percent of unaligned and short feathers did not explain variation in crest f_r, the repeatability of crest f_r was very high at 94%, suggesting that other characteristics may contribute to the consistent differences among individual crests.

The sharpness of the crest's resonant frequency is indicated by the quality factor, Q. The mean Q for peafowl crests vibrated in the out-of-plane orientation (grand mean 6.2 for males, 4.8 for females) was intermediate between those of peafowl eyespot feathers (Q = 3.6-4.5 ± 0.4 and 1.8 ± 0.3, for individual feathers and feather arrays, respectively) and the tail feathers that drive the shaking, for which Q_1 = 7.8 ± 0.5 (Dakin et al., 2016), indicating that peafowl crests are moderately-tuned resonators. The quality factor values also have implications for undriven vibrations, such as those caused by single gusts of air. These undriven vibrations take place at the crest's natural frequency, $f_o = f_r \, \mathrm{sqrt}(1 - \tfrac{1}{2} Q^{-2})$; this results in an undetectably small shift (≤ 1.2%) relative to measurement errors for our measured Q values of peafowl crests. We discuss the effect of this level of damping on the time behavior of feather vibrations below.

Approximately 49% of the variation in crest Q could be explained by sex, crest orientation, and the total area of the pennaceous flags (Fig. 2). Male crests were significantly more sharply-tuned

than those of females ($p < 0.0001$), and crests that had less flag area tended to be more sharply-tuned as well ($p = 0.03$). Peafowl crests also have more sharply-tuned resonance when they are vibrated out-of-plane ($p < 0.0001$) as compared to the in-plane orientation. The repeatability of Q was moderate, at 47%.

To determine the response of individual crest feathers, we removed all but three feathers (the two outermost and middle) for three of the crests studied above (two male and one female). The frequency response of individual feathers was generally consistent with that of the intact crests, as the average resonant frequency for individual male feathers was 26.88 [22.90, 30.87] Hz and 25.47 [18.52, 32.42] Hz for the female crest feathers. Additionally, this analysis revealed a sharp difference between single feathers that were aligned with the whole crest (where the direction of vibrational motion is out-of-plane) and those that were not aligned. The average resonance for the aligned feathers was 29.88 [27.36, 32.39] Hz in males and 27.16 [21.26, 33.07] Hz in females, whereas the unaligned feathers resonated at 21.89 [33.07, 21.26] Hz for the male crests and 22.09 [N/A] Hz for the females.

The average Δf was 4.81 [2.88, 6.75] Hz for male crests and 4.61 [0.66, 8.56] Hz for female crests. Just as for the resonance, there was a sharp divide between aligned and unaligned feathers after the majority of the crest feathers were removed. For the male crests, the aligned feather average was 6.35 [5.29, 7.42] Hz and the unaligned average was 2.25 [1.44, 3.07] Hz. The averages for the female crest feathers were 5.63 [5.33, 5.92] Hz and 2.59 [NA] Hz for aligned and unaligned, respectively.

Audio playback experiments

An example power spectrum for the vibrational response of a peahen crest during audio playback is shown in Fig. 3. For audio files played back at in the near-field of the speaker, the vibrational power spectra of the peafowl crests had a peak well above noise near the resonant frequency for all but the white noise signal, for which there was no measurable response above noise. In each case measured, the peak frequency of crest vibrations exceeded the resonant frequency of the crest by 4 ± 2 (male) to 4.5 ± 0.2 (female) Hz (mean ± SE). This shift toward higher frequencies was greater than the ≤ 0.3 Hz shift expected from the playback system's low frequency roll-off, but it was smaller on average than the width, Δf, of the crest's vibrational resonant response (90% Δf for female and 66-125% Δf for the male crest).

Wing-shaking experiments

The simulated wing-shaking experiment resulted in an airflow pattern with speeds ≤ 0.3 m/s. We used the measured positions of maximum airflow speed to determine the locations for three female crests for vibrational motion studies. Up to a maximum distance of approx. 90 cm (one sample) and 80 cm (two samples) from the mean wingtip position, the FFT power spectra of the crest flag vibrational motion resulted in a peak (Fig. 4) that agreed with the wing-shaking frequency within 95% CI. One crest had a lower power peak at the resonant frequency (29.0 ± 0.1 Hz vs. $f_r = 27.1 \pm 0.2$ Hz) for the greatest distances measured; a few samples also showed peaks with weak power at the first harmonic of the shaking frequency.

The average peacock wing-flapping frequency during ascending and level flight was 5.53 ± 0.30 Hz (mean ± SE) (Table S1). This frequency agrees with the average frequency of 5.4 Hz (range

4.5-6.9 Hz) found for wing-shaking display frequencies measured in the field (Dakin et al., 2016).

Air vortex experiments

When ring-shaped air vortices traveling at approx. 1.4 m/s impacted the crests, the barbs responded with clearly visible motion on video with the average amplitude of motion at the flags of 9.4 [4.3, 14.4] mm (Fig. 5A). Analysis of the free vibrational displacement of the crests over time revealed an exponentially decaying sinusoidal response with a frequency that agreed closely with the measured resonant frequency of each crest (Fig. 5B). Thus, vortices cause the feather crest to vibrate at its natural frequency, with a decrease in amplitude of approx. 13% after 0.2 s (the approx. period of peafowl wing-shaking displays).

We were unable to detect any forces above noise during either audio playbacks or vortex impact experiments, indicating that the forces exerted on the crests were ≤ 0.03 N.

Mechanical bending properties

All feather crests exhibited an elastic response in the bending experiments: force and displacement were linearly related for displacements up to 10.1 [9.1, 11.0] mm (adjusted R^2 = 0.983 [0.975, 0.990] for males, 0.984 [0.975, 0.993] for females), allowing us to compute the bending spring constant, k, from the fitted slopes (Fig. 6). The mean static bending spring constants for the individual crests ranged from 0.0022 to 0.0054 N/mm with a measurement repeatability of 47%. Two out of three male crests had values of k that were higher than any of the measurements for the peahen crests, but the difference between sexes in this small sample of 3 male and 3 female crests was not statistically significant (p = 0.09).

DISCUSSION

The findings from this study on peafowl point to a possible role of their feather crests for sensing airborne signals generated by their social motor displays. Morphometrics confirmed that the crests of different individual peafowl are relatively uniform in length and area, as previously found in live birds (Dakin, 2011). This structural uniformity helps explain their well-defined and narrow vibrational resonances (Fig. 2). We performed several different biomechanical experiments to understand whether the vibrational mechanics of peafowl crests were consistent with a sensory role. The fundamental resonant vibrational frequencies of peafowl crests agreed closely with the frequencies used during male train-rattling and female tail-rattling displays. This similarity seems unlikely to be due to coincidence, given the wide range of vibrational fundamental frequencies found for feathers of various lengths and structures in prior studies: for example, approx. 1 to 25 Hz in (Dakin et al., 2016) and ≥ 1 kHz in (Bostwick et al., 2009) and (Clark et al., 2013). This finding also indicates that peafowl crests can be driven efficiently by stimuli caused by their social displays. To further test this hypothesis, we examined the response of crests to audio playback of train-rattling sounds, and verified that train-rattling caused the crests to vibrate detectably near-resonance, whereas white noise resulted in no measurable vibrations above background noise levels.

Since there were no resonant modes of peafowl crests close to the 5 Hz frequency of peacock wing-shaking displays, we were interested to find that the wing-flapping motions used to simulate this display in the laboratory also resulted in crest deflections of several mm at a distance approx. 50 cm from the wing-tips. This implies that airflow impulses generated by the wing-shaking display can also stimulate the feather crests of nearby females. To understand the crest response at a frequency so far from resonance, we measured the deflection of peafowl crests when they were struck by individual air vortices. As expected from their relatively low values of quality factor, Q, we found that the crests vibrated near resonance only briefly and returned close to equilibrium after a time comparable to the period of peacock wing-shaking displays. Thus, the airflow due to wing-shaking constitutes a series of essentially distinct impulses that can drive detectable crest responses when air flow disturbances are of sufficient magnitude. One implication of this result is that hybrid biomimetic structures using a combination of feathers and resistance-based flex sensors provide a novel approach to making sensitive detectors for sensing impulsive or periodic airflows. Such devices are required for proposed robotic applications of air vortex rings and other airflow signals as a communication channel (Russell, 2011). Interestingly, peacocks also tilt their trains fore-and-aft during train-rattling at approx. 1 Hz, although we have not yet tested whether the airflows generated by these slower maneuvers can also influence the crest.

Static mechanical tests also showed that the peafowl feather crest flags deflected linearly with bending force. This indicates that the results measured for high magnitude airflows, sound pressure waves, and shaking forces can be extrapolated to the regime of lower-amplitude driving forces that might correspond to actual peafowl displays. This suggests that the magnitude of deflections found when feather crests were exposed to either wing-shaking or audio playbacks are not inconsistent with a sensory role, given that the combined effects of amplification via mechanical resonance and neural processes result in exquisitely small thresholds for animals that detect flows using mechanosensors. For example, in mammals, hair cells are sensitive to sub-nanometer displacements and 0.01 deg rotations (Crawford and Fettiplace, 1985), tactile receptors in human skin are sensitive to vibrational amplitudes well under a micron (Lo¨fvenberg and Johansson, 1984), pigeons can detect submicron threshold vibrational amplitudes applied to flight feathers (Hörster, 1990), and insect filiform hairs are sensitive to airspeeds as low as 0.03 mm s^{-1} (Shimozawa et al., 2003). Further histological and electrophysiological studies of the receptors at the base of avian crest feathers are needed to determine their sensitivity to the types of stimuli studied here.

The hypothesis that feathers might help detect airborne signals also suggests a new way to conceptualize behavioral experiments on birds that produce low frequency sound. Such studies have tended to assume that these signals can be reproduced suitably by a distant source. Indeed, greater distances often have been emphasized in experiments on signals emitted at low-frequencies because of their potential as an effective means of long-distance communication. For example, capercaillie males produce mechanical sound when they perform "flutter-jump" wing-shaking displays (Lieser et al., 2005). Experiments designed to study this behavior found no behavioral response when females were exposed to playbacks of the infrasound (< 20 Hz) component of flutter-jump recordings produced by speakers located 5 m away (Freeman and Hare, 2011; Lieser et al., 2006; Manley et al., 2011). In another study, peafowl were observed to perceive and respond behaviorally to playbacks of the infrasound

components of train-rattling and wing-shaking recordings using rotary subwoofers located 5-20 m away from the birds studied (Freeman and Hare, 2015). Behavioral studies of auditory thresholds indicate that that some bird species (chickens and pigeons, but not budgerigars or ducks) can detect low frequency sounds < 20 Hz with their ears (Heffner et al., 2013; Heffner et al., 2016; Hill, 2017; Hill et al., 2014); these studies also argue that eardrum perforation experiments prove that these birds lack the ability to detect sound by mechanosensory means. However, all of these studies probed only the far field given the experimental design. Thus, they were designed appropriately for determining the detection by hearing of the pressure-wave components of the acoustic signal, but not the effect of near-field airflow component on nearby receivers. It would be of great interest to study birds that produce sound with a low frequency component by vocal and mechanical means using near-field study designs. For example, cassowaries produce sound with fundamental frequencies of 23 or 32 Hz using vocalizations that make their entire bodies vibrate; humans are reported to both hear and feel these vibrations, suggesting that this sound likely produces tactile airflow or substrate vibration signals in conspecifics as well (Mack et al., 2003). In the future, audio playback experiments should be conducted in both the far- and near-fields to explore the possibility of such signals being transmitted via airflow rather than far-field pressure waves.

Peafowl are not the only bird species that have crests and perform shaking displays; for example, we have compiled a list of at least 35 species distributed over 10 avian orders (Table S2). Given that feathers function as airflow sensors during flight, it is easy to imagine how they could be co-opted to function as sensors during social signaling. Birds from diverse species spanning several orders are known to have filoplumes on their heads that extend past the contour feathers (Childress and Bennun, 2002; Clark and de Cruz, 1989; Imber, 1971; James, 1986). Many external stimuli and animal motions produce incidental sounds and airflows that could stimulate these feathers, and eventually be adapted to communicative uses. The congruence between peacock wingbeat frequencies in flight and during wing-shaking displays is consistent with this scenario. The sound and air-flow signals associated with such motions can be associated with kinematic parameters that may serve as signals of muscular performance, such as wingflap frequency, amplitude, and/or duration (Clark, 2016). One can also imagine hitherto unsuspected functions in addition to signal detection. For example, if feather crests allow birds to detect wind speed and direction, this could be useful for stabilization during flight or during roosting when the eyes are closed. Because predators that hunt by scent tend to approach prey from downwind, the ability to sense wind direction may be a useful anti-predator adaptation (Conover, 2007). Such a wind sensor should be flexible enough to provide sensitivity via detectable deformations for airflows in the range of interest, but rigid enough so its maximum bending occurs outside the range of typical airflow magnitudes. Many feather crests of birds meet these criteria. Of course, the fact that a particular species' feather crest is used for some function doesn't mean that its shape has evolved primarily in response to that function.

Our results raise the important question of whether peafowl respond behaviorally to near-field airflow signals detected by the crest. Further experiments could test this by removing or altering the crest and examining the effect on response to courtship displays, and/or performance during flight, roosting, and/or predator avoidance. One way to do this would be to paint the crest feathers with a clear varnish, because this should shift the resonant responses of the crest without changing its appearance visually or adding substantially to its mass. Other experimental

592 approaches might involve measuring the response of peafowl to puffs of air directed toward specific regions of their plumage, to see how this influences attention and body orientation.
594 Also, the airflow patterns generated by wing-shaking peacocks could be determined and compared to the movement of females during this display, to test whether specific female
596 movements are induced by male actions.

598 Thus far, the elaborate shape and size of bird feather crests has led to an emphasis on their visual appearance. Many avian courtship displays also involve wing-shaking, tail-fanning and
600 mechanical sound production that may be detected by nearby females in the vibrotactile channel (Table S2). Given the growing interest in multisensory signaling, it seems worth pursuing
602 behavioral studies to investigate the possibility of vibrotactile stimulation. For example, experiments have shown that that male African crickets signal to females using air vortices
604 produced by wing flicks that are detected by hair-like cerci (Heidelbach and Dambach, 1997; Heinzel and Dambach, 1987; Lunichkin et al., 2016). Other arthropods use mechanoreception
606 for predator or prey detection, and both insects and arachnids communicate via airflow tactile signals (Markl, 1983; Santer and Hebets, 2008; Steinmann and Casas, 2017). The close match
608 between the biomechanics of peafowl crests and peafowl social displays suggest that it is time to explore whether birds use their feathers for vibrotactile sensing in similar ways.
610

FIGURE LEGENDS

612

Fig. 1. Peafowl crest feathers have a morphology suitable for detecting mechanical signals
614 **during displays.** (A) A peahen (foreground) with the plane of her crest oriented towards the displaying peacock (background) as he performs train-rattling vibrations. (B) Both sexes have a
616 crest with an inverted pendulum shape made up of approx. 20-31 feathers. This photo shows an adult male measured *in vivo*. (C) A whole crest sample mounted for the laboratory experiments.
618 The two directions considered for vibrational motions (in and out of the crest plane) are indicated. (D) Morphology of the whole crest samples as compared to that of live peafowl
620 crests. Crests measured *in vivo* (shown to the right of the dried sample data) were similar to the dried samples, although on live birds the crests tended to be wider. Dried samples were
622 measured to the nearest 0.1 cm. (E) A single crest feather showing the pennaceous flag at the distal end. Note that only short, thin barbs are present on the relatively bare rachis (shaft) on the
624 proximal end.

626 **Fig. 2. Vibrational resonance properties of peafowl crests and individual crest feathers.** (A) Vibrational spectrum and Lorentzian fit for a peacock crest. (B) The resonant frequency, f_r,
628 of the crest is a close match for the range of vibrational frequencies used during peafowl social displays. As an indication of measurement error, the average 95% CI for each f_r estimate spans
630 0.072 Hz. The gray shaded area is the range of vibrational frequencies of the train-rattling display, with dotted lines showing the means for displays performed by peacocks (blue) and
632 peahens (green) (Dakin et al., 2016). Variation in f_r was influenced by the vibrational orientation and was also associated with the sex of the bird and the area of pennaceous flags at the top of the
634 crest (although the association with flag area was not statistically significant). (C) The quality factor, Q, was also influenced by the vibrational orientation, and was associated with the sex of
636 the bird and the area of pennaceous flags. The average 95% CI for each Q estimate spanned 0.233. Black horizontal lines in (B-C) are means.

Fig. 3. Effect of audio playback on crests. Vibrational response of a peahen crest exposed to peacock train-rattling audio playbacks in the near-field of the speaker. The FFT spectral power for the peahen crest during playbacks peaked near the resonant frequency of the crest.

Fig. 4. Effects of simulated wing-shaking displays. Vibrational response of a female peahen crest exposed to airflow from a robot that simulated 5.0 Hz peacock wing-shaking displays at a distance 50 cm from the moving wingtip (Fig. S2).

Fig. 5. Displacement of the crest in response to air vortices. (A) Time series showing the change in flag position after a peacock crest is impacted by a vortex of air created by a gun. When peafowl crests were impacted by air ring vortices, they deflected measurably, oscillating at their resonant frequency with an amplitude that decayed to a few percent of the initial value over the period of the peacock's wing-shaking display. (B) Resonant frequencies (f_r) and vortex response frequencies (± 95% CI) for three crests in the vortex experiment.

Fig. 6. Mechanical properties of the crests of male and female peafowl. (A) Bending spring constant, k, for peahen and peacock crests. Each crest was tested three times and is denoted by a different shape symbol. The horizontal lines are the grand mean for each sex. (B-D) Variation in the spring constant was not explained by rachis length, number of feathers, or the area of pennaceous flags.

Acknowledgments

We thank Robert Beyer, Maarten Hesseling, Robert Lukasik, Roger Hill, Kathy Kerran, and Jim Hare.

Competing interests

The authors declare no competing or financial interests.

Author contributions

Conceptualization: S.A.K.; Methodology: S.A.K., D.V.; Investigation: S.A.K., D.V.; Data curation: S.A.K., D.V., R.D.; Analysis: S.A.K., R.D., D.V.; Writing – original draft: S.A.K., R.D.; Writing – review & editing: S.A.K., R.D., D.V.

Funding

This work was supported by Haverford College and a National Sciences and Engineering Research Council of Canada (NSERC) Postdoctoral Fellowship to R.D.

Data availability

Data and analysis are available from Figshare at: https://figshare.com/s/24beee4b025388e3e297

References

Alibardi, L. (2009). Follicular patterns during feather morphogenesis in relation to the formation of asymmetric feathers, filoplumes and bristles. *Ital. J. Zool.* **76**, 279–290.

Barth, F. G. (2014). The Slightest Whiff of Air: Airflow Sensing in Arthropods. In *Flow Sensing in Air and Water*, pp. 169–196. Springer, Berlin, Heidelberg.

Barth, F. G., Humphrey, J. A. C. and Srinivasan, M. V. (2012). *Frontiers in Sensing: From Biology to Engineering*. Springer Science & Business Media.

Bartoń, K. (2015). *MuMIn 1.15.6*.

Bilo, D. and Bilo, A. (1978). Wind stimuli control vestibular and optokinetic reflexes in the pigeon. *Naturwissenschaften* **65**, 161–162.

Bostwick, K. S., Elias, D. O., Mason, A. and Montealegre-Z, F. (2009). Resonating feathers produce courtship song. *Proc. R. Soc. Lond. B Biol. Sci.* rspb20091576.

Bradbury, J. W. and Vehrencamp, S. L. (2011). *Principles of Animal Communication*. Sinauer.

Brown, R. E. and Fedde, M. R. (1993). Airflow sensors in the avian wing. *J. Exp. Biol.* **179**, 13–30.

Brücker, C., Schlegel, D. and Triep, M. (2016). Feather vibration as a stimulus for sensing incipient separation in falcon diving flight. *Nat. Resour.* **7**, 411.

Burley, N. T. and Symanski, R. (1998). "A taste for the beautiful": Latent aesthetic mate preferences for white crests in two species of Australian grassfinches. *Am. Nat.* **152**, 792–802.

Butler, J. M. and Maruska, K. P. (2016). Mechanosensory signaling as a potential mode of communication during social interactions in fishes. *J. Exp. Biol.* **219**, 2781–2789.

Childress, R. B. and Bennun, L. A. (2002). Sexual character intensity and its relationship to breeding timing, fecundity and mate choice in the great cormorant *Phalacrocorax carbo lucidus*. *J. Avian Biol.* **33**, 23–30.

Clark, C. J. (2016). Locomotion-induced sounds and sonations: mechanisms, communication function, and relationship with behavior. In *Vertebrate Sound Production and Acoustic Communication*, pp. 83–117. Springer, Cham.

Clark, G. A. and de Cruz, J. B. (1989). Functional interpretation of protruding filoplumes in oscines. *The Condor* **91**, 962–965.

Clark, C. J., Elias, D. O., Girard, M. B. and Prum, R. O. (2013). Structural resonance and mode of flutter of hummingbird tail feathers. *J. Exp. Biol.* **216**, 3404–3413.

Conover, M. R. (2007). *Predator-Prey Dynamics: The Role of Olfaction*. CRC Press.

Crawford, A. C. and Fettiplace, R. (1985). The mechanical properties of ciliary bundles of turtle cochlear hair cells. *J. Physiol.* **364**, 359–379.

Cummins, B. and Gedeon, T. (2012). Assessing the Mechanical Response of Groups of Arthropod Filiform Flow Sensors. In *Frontiers in Sensing*, pp. 239–250. Springer, Vienna.

Cunningham, S. J., Alley, M. R. and Castro, I. (2011). Facial bristle feather histology and morphology in New Zealand birds: Implications for function. *J. Morphol.* **272**, 118–128.

Dakin, R. (2011). The crest of the peafowl: a sexually dimorphic plumage ornament signals condition in both males and females. *J. Avian Biol.* **42**, 405–414.

Dakin, R. and Montgomerie, R. (2009). Peacocks orient their courtship displays towards the sun. *Behav. Ecol. Sociobiol.* **63**, 825–834.

Dakin, R., McCrossan, O., Hare, J. F., Montgomerie, R. and Kane, S. A. (2016). Biomechanics of the peacock's display: How feather structure and resonance influence multimodal signaling. *PLOS ONE* **11**, e0152759.

Dakin, R., van Beveren, D. and Amador Kane, S. (2017). Statistical supplement to: Biomechanics of the peafowl's crest: a potential mechanosensory role for feathers during social displays.

Dambach, M., Rausche, H.-G. and Wendler, G. (1983). Proprioceptive feedback influences the calling song of the field cricket. *Naturwissenschaften* **70**, 417–418.

Davis, A., Bouman, K. L., Chen, J. G., Rubinstein, M., Durand, F. and Freeman, W. T. (2015). Visual vibrometry: estimating material properties from small motion in video.pp. 5335–5343.

Fletcher, N. H. (1992). *Acoustic Systems in Biology*. Oxford University Press.

Fournier, J. P., Dawson, J. W., Mikhail, A. and Yack, J. E. (2013). If a bird flies in the forest, does an insect hear it? *Biol. Lett.* **9**, 20130319.

Freeman, A. R. and Hare, J. F. (2011). Infrasound in the flutter-jump display of Capercaillie (*Tetrao urogallus*): signal or artefact? *J. Ornithol.* **152**, 815–816.

Freeman, A. R. and Hare, J. F. (2015). Infrasound in mating displays: a peacock's tale. *Anim. Behav.* **102**, 241–250.

Garcia, M., Charrier, I. and Iwaniuk, A. N. (2012). Directionality of the drumming display of the ruffed grouse. *The Condor* **114**, 500–506.

Hagelin, J. C. (2002). The kinds of traits involved in male—male competition: a comparison of plumage, behavior, and body size in quail. *Behav. Ecol.* **13**, 32–41.

Hart, N. S. (2002). Vision in the peafowl (Aves: *Pavo cristatus*). *J. Exp. Biol.* **205**, 3925–3935.

Heffner, H. E., Koay, G., Hill, E. M. and Heffner, R. S. (2013). Conditioned suppression/avoidance as a procedure for testing hearing in birds: The domestic pigeon (*Columba livia*). *Behav. Res. Methods* **45**, 383–392.

Heffner, H. E., Koay, G. and Heffner, R. S. (2016). Budgerigars (*Melopsittacus undulatus*) do not hear infrasound: the audiogram from 8 Hz to 10 kHz. *J. Comp. Physiol. A* **202**, 853–857.

Heidelbach, J. and Dambach, M. (1997). Wing-flick signals in the courtship of the African cave cricket, *Phaeophilacris spectrum*. *Ethology* **103**, 827–843.

Heinzel, H.-G. and Dambach, M. (1987). Travelling air vortex rings as potential communication signals in a cricket. *J. Comp. Physiol. A* **160**, 79–88.

Hill, E. M. (2017). Audiogram of the mallard duck (*Anas platyrhynchos*) from 16 Hz to 9 kHz. *J. Comp. Physiol. A* 1–6.

Hill, E. M., Koay, G., Heffner, R. S. and Heffner, H. E. (2014). Audiogram of the chicken (*Gallus gallus domesticus*) from 2 Hz to 9 kHz. *J. Comp. Physiol. A* **200**, 863–870.

Hingee, M. and Magrath, R. D. (2009). Flights of fear: a mechanical wing whistle sounds the alarm in a flocking bird. *Proc. R. Soc. Lond. B Biol. Sci.* rspb20091110.

Hörster, W. (1990). Vibrational sensitivity of the wing of the pigeon (*Columba livia*) — a study using heart rate conditioning. *J. Comp. Physiol. A* **167**, 545–549.

Imber, M. J. (1971). Filoplumes of petrels and shearwaters. *N. Z. J. Mar. Freshw. Res.* **5**, 396–403.

James, P. C. (1986). The filoplumes of the Manx Shearwater *Puffinus puffinus*. *Bird Study* **33**, 117–120.

Jones, I. L. and Montgomerie, R. (1992). Least auklet ornaments: do they function as quality indicators? *Behav. Ecol. Sociobiol.* **30**, 43–52.

Kämper, G. and Dambach, M. (1981). Response of the cercus-to-giant interneuron system in crickets to species-specific song. *J. Comp. Physiol.* **141**, 311–317.

Larsen, O. N. and Wahlberg, N. (2017). Sound and Sound Sources. In *Comparative Bioacoustics: An Overview* (ed. Brown, C.) and Riede, T.), pp. 3–61. Sharjah, UAE: Bentham Science Publishers.

Lieser, M., Berthold, P. and Manley, G. A. (2005). Infrasound in the capercaillie (*Tetrao urogallus*). *J. Ornithol.* **146**, 395–398.

Lieser, M., Berthold, P. and Manley, G. A. (2006). Infrasound in the flutter jumps of the capercaillie (*Tetrao urogallus*): apparently a physical by-product. *J. Ornithol.* **147**, 507–509.

Lo¨fvenberg, J. and Johansson, R. S. (1984). Regional differences and interindividual variability in sensitivity to vibration in the glabrous skin of the human hand. *Brain Res.* **301**, 65–72.

Lucas, A. M. and Stettenheim, P. R. (1972). Structure of Feathers. In *Avian Anatomy: Integument*, pp. 341–419. Washington, DC: US Department of Agriculture.

Lunichkin, A. M., Zhemchuzhnikov, M. K. and Knyazev, A. N. (2016). Basic elements of behavior of the cricket *Phaeophilacris bredoides Kaltenbach* (Orthoptera, Gryllidae). *Entomol. Rev.* **96**, 537–544.

Mack, A. L., Jones, J. and Nelson, D. A. (2003). Low-frequency vocalizations by cassowaries (casuarius spp.). *The Auk* **120**, 1062–1068.

Manley, G. A., Lieser, M. and Berthold, P. (2011). Studies of infrasound production and perception by the Capercaillie (*Tetrao urogallus*): a reply to Freeman and Hare. *J. Ornithol.* **152**, 817–818.

Markl, H. (1983). Vibrational Communication. In *Neuroethology and Behavioral Physiology*, pp. 332–353. Springer, Berlin, Heidelberg.

Mooney, T. A., Kaplan, M. B. and Lammers, M. O. (2016). Singing whales generate high levels of particle motion: implications for acoustic communication and hearing? *Biol. Lett.* **12**, 20160381.

Nakagawa, S. and Schielzeth, H. (2010). Repeatability for Gaussian and non-Gaussian data: a practical guide for biologists. *Biol. Rev.* **85**, 935–956.

Nakagawa, S. and Schielzeth, H. (2013). A general and simple method for obtaining R2 from generalized linear mixed-effects models. *Methods Ecol. Evol.* **4**, 133–142.

Necker, R. (1985). Observations on the function of a slowly-adapting mechanoreceptor associated with filoplumes in the feathered skin of pigeons. *J. Comp. Physiol. A* **156**, 391–394.

Ota, N., Gahr, M. and Soma, M. (2015). Tap dancing birds: the multimodal mutual courtship display of males and females in a socially monogamous songbird. *Sci. Rep.* **5**,.

Persons, W. S. and Currie, P. J. (2015). Bristles before down: A new perspective on the functional origin of feathers. *Evolution* **69**, 857–862.

Pinheiro, J., Bates, D., DebRoy, S. and Sarkar, D. (2017). *nlme 3.1-131: linear and nonlinear mixed effects models*.

R Core Team (2017). *R 3.3.3: A Language and Environment for Statistical Computing*. Vienna, Austria: R Foundation for Statistical Computing.

Russell, R. A. (2011). Air vortex ring communication between mobile robots. *Robot. Auton. Syst.* **59**, 65–73.

Santer, R. D. and Hebets, E. A. (2008). Agonistic signals received by an arthropod filiform hair allude to the prevalence of near-field sound communication. *Proc. R. Soc. Lond. B Biol. Sci.* **275**, 363–368.

Saxod, R. (1978). Development of Cutaneous Sensory Receptors Birds. In *Development of Sensory Systems*, pp. 337–417. Springer, Berlin, Heidelberg.

Seneviratne, S. S. and Jones, I. L. (2008). Mechanosensory function for facial ornamentation in the whiskered auklet, a crevice-dwelling seabird. *Behav. Ecol.* **19**, 784–790.

Seneviratne, S. S. and Jones, I. L. (2010). Origin and maintenance of mechanosensory feather ornaments. *Anim. Behav.* **79**, 637–644.

Shimozawa, T., Murakami, J. and Kumagai, T. (2003). Cricket wind receptors: thermal noise for the highest sensitivity known. In *Sensors and Sensing in Biology and Engineering*, pp. 145–157. Springer, Vienna.

Smith, W. F. (2010). *Waves and Oscillations: A Prelude to Quantum Mechanics*. Oxford University Press.

Sofroniew, N. J. and Svoboda, K. (2015). Whisking. *Curr. Biol.* **25**, R137–R140.

Steinmann, T. and Casas, J. (2017). The morphological heterogeneity of cricket flow-sensing hairs conveys the complex flow signature of predator attacks. *J. R. Soc. Interface* **14**, 20170324.

Yorzinski, J. L., Patricelli, G. L., Babcock, J. S., Pearson, J. M. and Platt, M. L. (2013). Through their eyes: selective attention in peahens during courtship. *J. Exp. Biol.* **216**, 3035–3046.

Figure 1

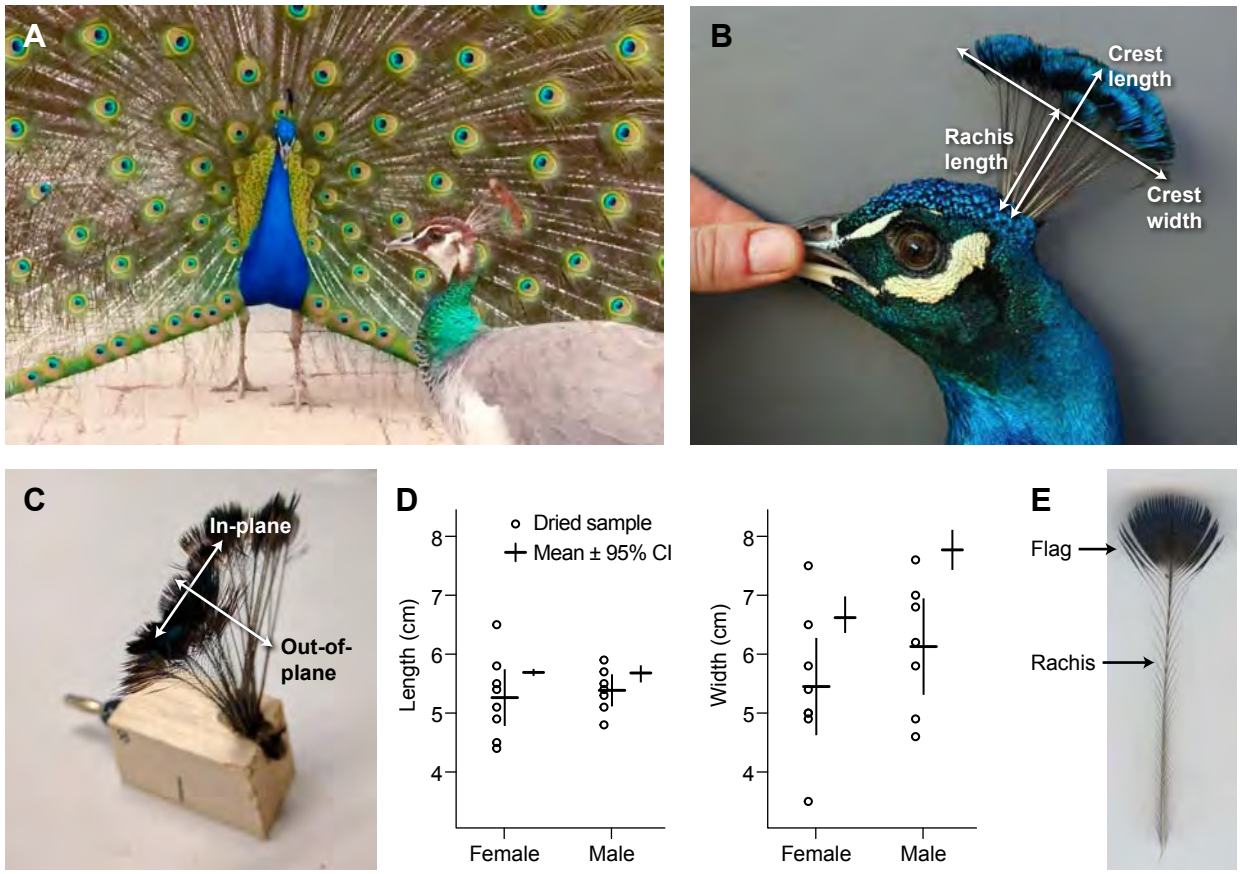

Figure 2

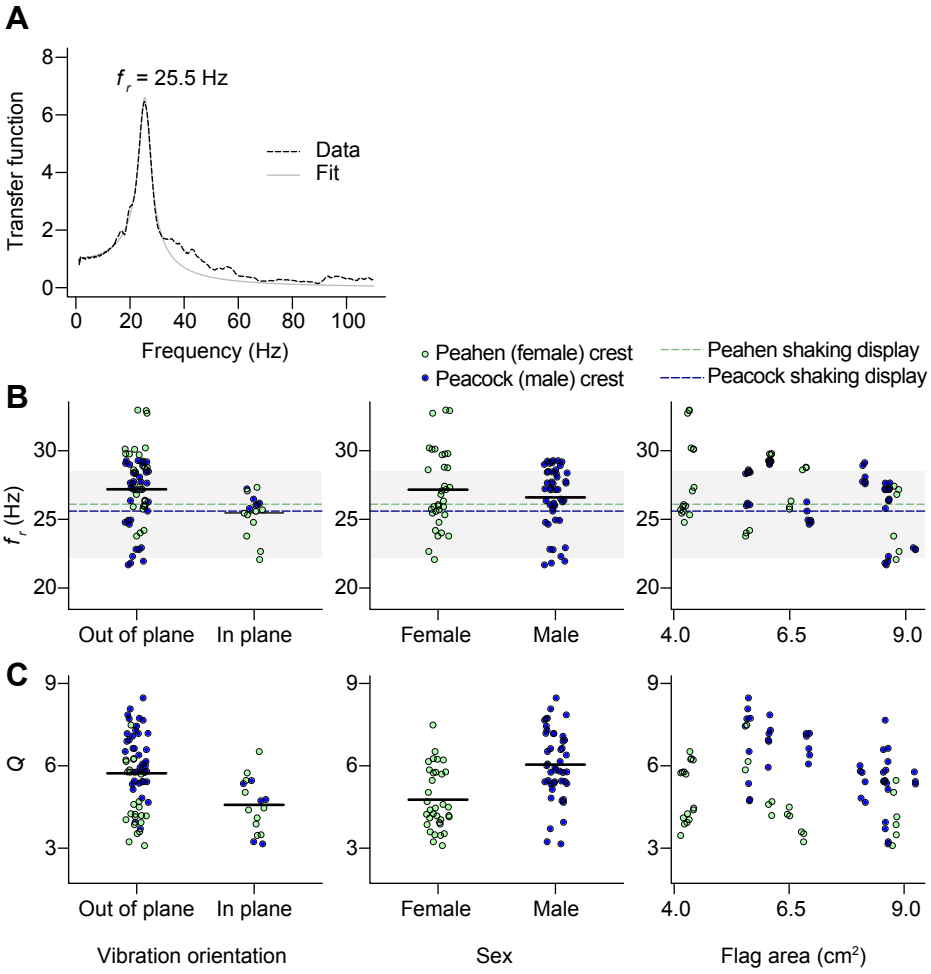

Figure 3

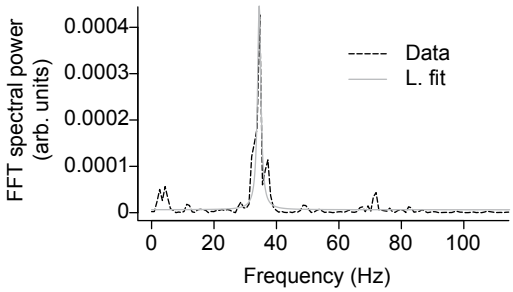

Figure 4

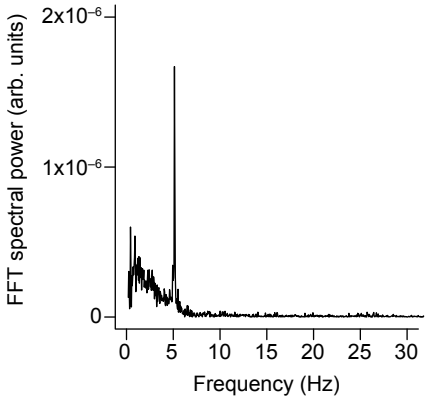

Figure 5

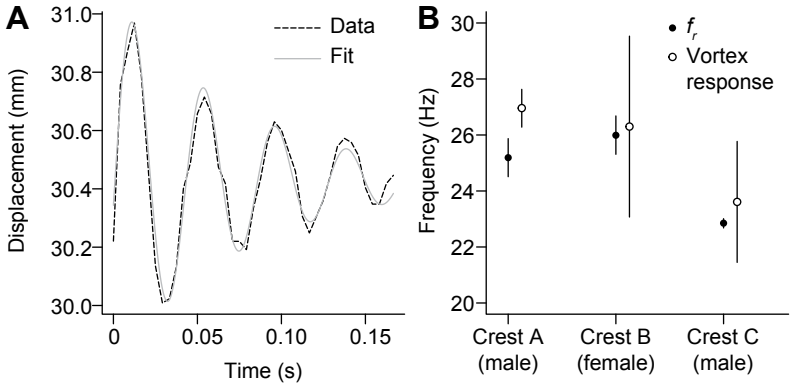

Figure 6